Geotech Geol Eng
https://doi.org/10.1007/s10706-024-02892-4

ORIGINAL PAPER

Geotechnical Insights of the Cut Slopes Along Silchar-Haflong National Highway, Assam, India

Ratan Das · T. N. Singh

Received: 9 May 2024 / Accepted: 17 July 2024

Abstract Insufficient geological research and a limited understanding of ground conditions during the design phase often led to slope failures and subsequent repair costs. This issue is notable in the 104 km Silchar-Haflong National Highway in Assam, India, located in the northwestern part of the Assam-Arakan folded mountain range. Over 158 slope failures have occurred due to various geo-climatic factors aggravated by human activities. A comprehensive engineering geological investigation was conducted on a 25 km section, using techniques like RMR_{basic}, SMR, Q_{slope} to assess slope conditions at several locations. Stability analyses were carried out using finite element numerical method for both dry and saturated conditions, revealing four potentially unstable slopes (L3, L5, L7, and L8). Critical SRF values ranged from 1.15 to 1.72 for dry conditions, while they varied from 0.95 to 0.98 for saturated conditions. The study also examined rockfall analysis for slope L7, considering parameters such as translational velocity, rebound height, kinetic energy, and travel distance. The findings indicated a potential for falling blocks to reach the road and pose a significant risk. The study emphasizes the need for implementing appropriate measures to address informal slope excavation, or else there is a likelihood of increased frequency and scale of rainfall-triggered roadside slope failures.

Keywords Slope condition · Silchar-Haflong highway · Rainfall · Failure

R. Das (✉)
Rock Mechanics and Rock Engineering Laboratory, Department of Geology, Cotton University, Guwahati, Assam 781001, India
e-mail: ratan.das@cottonuniversity.ac.in

T. N. Singh
Department of Civil and Environmental Engineering, Indian Institute of Technology, Patna, Bihar 801106, India
e-mail: director@iitp.ac.in

1 Introduction

The landslides are the downslope movement of rock, debris, or soil due to gravitational pull triggered by a variety of external factors such as heavy rainfall, earthquake, etc., resulting in significant economic loss and infrastructure damage (Hungr et al. 1999; Singh et al. 2016a; Yang et al. 2020). The highway projects carry higher risk than other construction projects as they entail high capital outlays and intricate site conditions (Tawalare 2019). The highway networks are essential for a nation's development and economic growth. However, frequent cut slope failures due to natural calamities and human interventions cause trouble throughout the road network. Unfortunately, in India, even today, expenses over geotechnical investigations are considered unnecessary; hence, funding is typically meager, often amounting to less than 1% of overall construction expenses. In cut-slope construction, ground investigation costs are generally

Published online: 31 July 2024

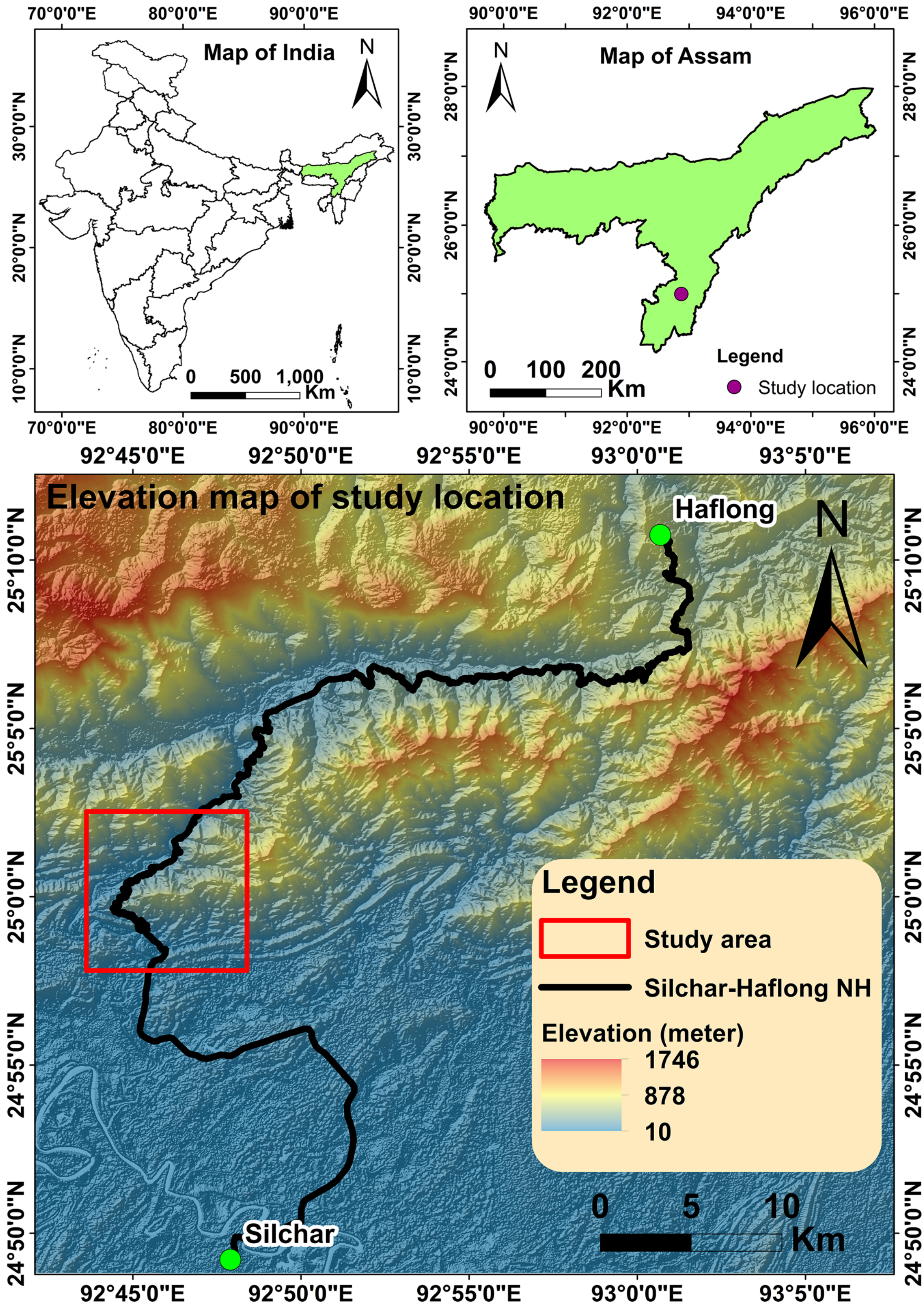

Map of India
N
0 500 1,000
Km
70°0'0"E
80°0'0"E
90°0'0"E
10°0'0"N
20°0'0"N
30°0'0"N
Map of Assam
N
0 100 200
Km
Legend
Study location
90°0'0"E
92°0'0"E
94°0'0"E
96°0'0"E
24°0'0"N
26°0'0"N
28°0'0"N
Elevation map of study location
Haflong
Silchar
N
Legend
Study area
Silchar-Haflong NH
Elevation (meter)
1746
878
10
0 5 10
Km
92°45'0"E
92°50'0"E
92°55'0"E
93°0'0"E
93°5'0"E
24°50'0"N
24°55'0"N
25°0'0"N
25°5'0"N
25°10'0"N

◂**Fig. 1** Elevation map showing the study area (red box) along Silchar-Haflong highway (Data from "NASA, SRTM 2013": https://portal.opentopography.org/)

lower and are sometimes omitted altogether (Lee and Hencher 2009). Unanticipated geological conditions arising from insufficient research can lead to cost escalations in projects by 10% or more (Paniagua et al. 2021). The limited financial commitment and suboptimal quality of investigations result in geological and hydrogeological models of cut-slope stability during the design phase are rarely realistic. Additionally, post-failure investigations are often superficial, leading to incorrect identification of the actual failure mechanisms. Consequently, failures are frequently misattributed to unforeseen geological factors rather than flaws in the cut-slope excavation design. This misattribution compels the client to bear the costs of remedial measures, ultimately inflating the overall project expenditure. Therefore, understanding the mechanism of rock cut slope failure and its vital aspects has progressed gradually over the years (Thuro and Eberhardt 2001; Korup 2005; Sengupta et al. 2010; Bera et al. 2019).

Though landslides are the results of combined effect of geological, hydro-meteorological, geomorphological and tectonic factors, the rainfall-induced landslides have got a lot of attention in the international literature during the last few decades (Crosta and Frattini 2008). Many experimental and numerical studies have looked at the impact of individual exogenetic processes on rock slope failure (Siddique et al. 2017; Siddque and Pradhan 2018; Singh and Kumar 2020; Jaiswal et al. 2023). But only a few research dealt with the influence of collective impact of different exogenetic processes on rock failure behavior. Generally, rock slope failure occurs due to the interplay between factors such as rock discontinuities, slope geometry, rock type, and the presence of moisture in the slope material. In most cases, the rock slope failure is controlled by water content variation due to rainfall (Iverson 2000; Dhar and Nandargi 2004; Guzzetti et al. 2008; Sengupta et al. 2010; Kanungo and Sharma 2014; Sanzeni et al. 2019), thermal effects (Pinyol et al. 2018; Shan et al. 2021; Loche et al. 2022), porewater pressure (Mesri and Shahien 2003; Wang and Sassa 2003; Mesri and Huvaj-Sarihan 2012), stressed rock (Gipprich et al. 2008), etc. Also, the presence of low-shear strength clay along the bedding surfaces of rocks can cause large, devastating landslides (Stead 2016; Singh et al. 2016a). All these conditions together invariably affect the ground destabilizing process, which is very important for planning safe slope design, slope health monitoring, and predicting the rock response for the design of highways, and other infrastructures.

It is noticed that many landslides occur along the road cut slopes in southern Assam, India triggered by incessant rainfall and earthquakes. None of the highways are free of such hazards and a majority of them are linked to difficult terrain condition particularly, the 104 km long Silchar-Haflong mountain highway (Fig. 1) that connects Guwahati and Dibrugarh city with Mizoram state via Silchar town in Assam (India). This route is often disrupted due to frequent landslides in the weak stratified Tertiary sedimentary rocks (Roy et al. 2023). The Dima Hasao district was found to be most vulnerable to landslide hazards in the Indian state of Assam. Roy et al. (2023) reported many landslides in the hilly regions of Haflong, Maibang, and Mahul of Dima Hasao triggered by antecedent rainfall during May 2022. The sedimentary strata occurred in these regions overlay the weathered platforms of Precambrian rocks, consisting of sedimentary deposits from the Palaeocene-Eocene period, encompassing both shelf and geosynclinal facies, which are represented by the Jaintia and Disang Groups, respectively (GSI 2019). Rainwater infiltration causes increase in the soil pore pressures, has led to frequent shallow landslides and debris flows on steep slopes, causing significant damage to this route. As landslides occur without warning, their direct impact has long been a major socioeconomic issue in this region and annually, the government allocates substantial funds and resources for restoration work in landslide-affected areas. These issues often isolate Silchar town, Tripura, and Mizoram from the rest of the country. The region remains scientifically unexplored and geotechnically overlooked; therefore, understanding the rock failure behavior is one of the fundamental requirements for safe construction of civil structures in the region. Therefore, a comprehensive understanding of the interactions between various geogenic and exogenic factors with rock slope failure is crucial..

This research investigated evidence-based components such as landslide-rainfall thresholds and geological conditions for risk assessment to understand the region's recurring landslide problem. The field investigation and laboratory geotechnical results were analyzed to evaluate the influence of climatic and geological conditions on rock mass strength and failure mechanisms. Numerical simulations were conducted to predict slope failure at specific locations within the study area, and to validate recent rockfall mechanisms. The findings will significantly contribute to safer slope design, slope health monitoring, and the prediction of rock failure responses, aiding in the design of highways, tunnels, bridges, and other infrastructure.

2 Study Area

2.1 Geological Setting

The Silchar-Haflong road section exposes ~ 7.5 km thick Tertiary sedimentary sequences of the fold belt of the Assam-Arakan basin. Along the road, there are exposures of deepwater Disang Shales, Barail Group (Laisong, Jenam, Renji formations), conglomerate representing the Oligocene Barail-Surma unconformity, entire Surma Group (Lower, Middle & Upper Bhuban and Bokabil shales), Tipam Group, followed by Dupitila Formation (equivalent of Namsang Formation) and recent Dihing Group (Fig. 2). The details of the datasets used in this study are given in. Table 1.

Tectonically, the Silchar-Haflong road section of Cachar district of Assam forms a small part of the frontal folded belt of Assam-Arakan folded mountain belt. Structurally, this area is distinguished by a

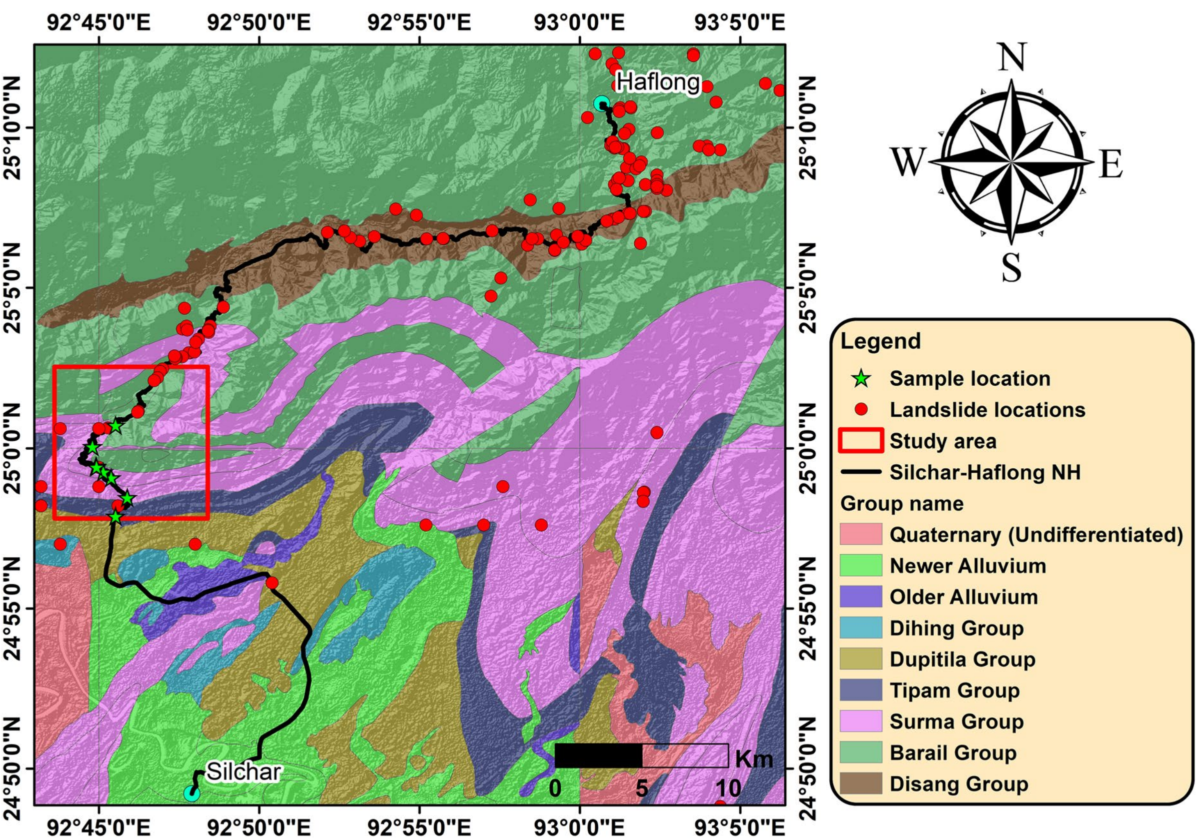

Fig. 2 Geological map of the study area draped on topographic data displaying past landslide distribution along with the locations of the investigated road cut slopes on the Silchar-Haflong National highway (Data from "Bhukosh")

Table 1 The dataset used in this study

Data type	Source	Special/temporal resolution	Data derived
Digital elevation model (DEM)	NASA, SRTM 2013 https://portal.opentopography.org/	30×30	Topography, slope map, aspect map of the area
Rainfall data	NASA, (POWER, Data access viewer) https://power.larc.nasa.gov/data-access-viewer/	Monthly average / annual precipitation	Temporal analysis of rainfall data
Geological map (shapefile)	Bhukosh https://bhukosh.gsi.gov.in/		Geological map, lithology, landslide inventory
Field investigation	On-site field study		Lithological study, sample collection, measurements of bed/discontinuity attitudes, etc

sequence of N-S to NNE-SSW trending arc-shaped, elongated, doubly plunging, and asymmetric folds organized in an en-echelon pattern, with a slight curvature towards the west (Ganguly 1983, 1984; Alam Laskar and Phukon 2013). The intensity of folding of these stratified rocks increases towards east as it approaches the Arakan-Yoma collision zone (Nandy 2001). The stratified rocks present in the region consist of alternation of sandstone, shale, sandy/silty shales, clayey sandstone and occasional impersistent bands of conglomerates and the exogenetic processes continually affect the failure behavior of rocks by influencing their hydromechanical and geomechanical properties (Singh et al. 2016a). The inclination of bedding layers and the mechanical characteristics of these bedding planes influence the strength and stability of rock masses (Singh et al. 2017; Tang et al. 2017). Consequently, evaluating the stability of slopes in stratified rock formations is intricate due to the prevailing discontinuities, which result in pronounced anisotropic behavior.

Based on the local geology and type of movement, majority of the mass movements of the study area can be categorized as “slide type” i.e., the downslope movement of a soil or rock mass that occurs on rupture surfaces or on relatively narrow zones of intense shear strain. During monsoon the uppermost layer of debris or soil becomes completely saturated, resulting in elevated pore water pressure. This, in turn, diminishes the material’s shear strength. If shear failure initiates, the unconsolidated material rapidly loses its strength and begins to flow (Fang et al. 2012; Das et al. 2022).

2.2 Geomorphology and Climatology of the Area

Part of the road section falls under Cachar district, and the rest section falls under Dima Hasao district of Assam. The block between the Haflong-Disang thrust and the probable fault south of it has been faulted into smaller blocks by connecting splays forming a contractional strike-slip duplex (Alam Laskar and Phukon 2013). The Silchar-Haflong national highway passes through one of these contractional strike-slip duplexes. The area consists of Barail range in the north, Bhuban and Manipur hills in the east, the Mizoram fold belt in the south, and the Bangladesh plains in the west. On average, the elevation rises in the north and east, reaching heights exceeding 1700 m above mean sea level (AMSL). Nonetheless, there’s a disparity in the orientation of the hill ranges, with the Barail range exhibiting an east-west alignment, whereas the southern hills extending across the Barak valley and the Manipur-Mizoram border follow a N-S to NNE to SSW pattern. The region features six principal landform characteristics: anticlinal hills, linear ridges, strike valleys, denudational hills, fluvial terraces, alluvial plains, and active floodplains.

Both districts are under the southwest monsoon’s direct influence and generally receive high annual rainfall, as inferred from the India Meteorological Department (IMD) (Guhathakurta et al. 2020). The districts are mostly made up of plains, but there are many structural hills spread across the districts. Based on rainfall data for the past 30 years i.e. 1989–2018, IMD calculated that the Cachar district receives an average annual rainfall of 2939.2 mm, while the Dima

Hasao district receives 2071.4 mm (Guhathakurta et al. 2020). Frequent heavy rainfall events during the monsoon period in geologically young and steep mountainous regions create saturated conditions which result in the reduction of shear strength and the increase of pore water pressure that decreases the ability of the slope to resist gravitational influence, especially in areas with poor surface drainage and highly sheared/weathered rocks.

3 Data and Methods

3.1 Field Investigation

The stability assessment of road cut slope is essential to slope engineering (Siddique et al. 2020). During the reconnaissance survey, most of the rocks encountered along the Silchar-Haflong national highway are alternate sandstone, shale, and siltstone that are prone to landslides due to their critical bedding attitudes and fragile nature (Table 2). Therefore, looking at the similar condition of exposed rocks, eight road cut sections were selected for a comprehensive geotechnical study out of which four (L3, L5, L7, and L8) were deemed to be vulnerable to failure (Fig. 3). The rock mass in some of the studied location were highly jointed resulting in the formation of rock blocks causing occasional rockfalls (Fig. 3g), therefore, a detailed study of the discontinuities was carried out viz. orientation, persistence, infilling, aperture, and seepage conditions. Geotechnical precautions such as retaining walls and suitable ditches are also noticeably absent in a significant section of the analyzed cut slopes. Comprehensive assessment and the implementation of precise remediation strategies are crucial for addressing the acute instability of these cut slopes.

3.2 Rock Mass Classification

Characterizing rock mass is an essential step in determining its geoengineering behavior. A well-known approach for the characterization of rock mass is RMR system that includes six rating parameters such as uniaxial compressive strength (UCS) (ASTM D7012-23 2023), rock quality designation (RQD), mean discontinuity spacing (DS), conditions of discontinuities (DC), groundwater condition, and an adjustment factor for discontinuity orientation (DO) (Eq. 1) (see Bieniawski 1989 for details).

$$RMR = (UCS + RQD + DS + CD + GW) - DO \quad (1)$$

$$RMR_{basic} = (UCS + RQD + DS + CD + GW) \quad (2)$$

Here, RQD is a standard technique for the qualitative and quantitative assessment of rock quality and degree of jointing and fracturing in a rock mass (Deere 1964) and can be expressed as the following Eq. (3):

$$RQD(\%) = \frac{\sum (length\ of\ core\ pieces \geq 0.10m)}{(Total\ length\ of\ core\ run)} \times 100 \quad (3)$$

In this study, RMR_{basic} (sum of ratings of the initial five parameters of RMR (Eq. 2)) has been further used to compute Slope Mass Raring (SMR) (Table 3).

Table 2 Investigated slope, rock type, and the overall geometry

Slope	Latitude	Longitude	Slope height (m)	Overall slope dip	Slope dip direction	Rock type/weathering condition
L1	24°57′52.43″ N	92°45′31.38″ E	32	85°	275°	Sandstone and conglomerate
L2	24°58′27.52″ N	92°45′53.41″ E	20	65°	190°	Loose debris material
L3	24°59′04.46″ N	92°45′23.10″ E	18	80°	200°	Weak sandstone
L4	24°59′15.52″ N	92°45′8.34″ E	25	75°	250°	Weathered sandstone
L5	24°59′20.35″ N	92°45′03.05″ E	24	80°	310°	Weak siltstone
L6	24°59′24.89″ N	92°44′55.86″ E	28	78°	165°	Jointed massive sandstone
L7	24°59′26.24″ N	92°44′54.88″ E	17	70°	200°	Near horizontal sandstone beds with orthogonal joint sets
L8	25°00′42.38″ N	92°45′31.50″ E	17	82°	225°	Sandstone beds dipping towards slope at high angle

Fig. 3 Field photographs depicting present-day rock mass condition along the Silchar-Haflong NH, **a** Polymictic conglomerate of Dupitila Formation at the top and massive medium-grained Tipam sandstone at the bottom, **b** Loose and weathered debris material, **c** Bhuban sandstone with daylight bedding planes, **d** Recently exposed cut slope in Bhuban sandstone, **e** very weak and friable Bhuban shale with bedding plane dipping towards the slope, **f** recently excavated road cut slope in Bhuban sandstone, **g** view of rockfall (sandstone blocks), **h** thinly bedded hard massive Barail sandstone dipping towards towards slope face

The SMR is obtained by subtracting adjustment factors (F1, F2, and F3) of the joint–slope relationship from RMR_{basic} and adding a factor depending on the method of excavation (F4), (more details can be found in (Romana 1985)) (Eq. (4)).

$$SMR = RMR_{basic} + (F_1.F_2.F_3) + F_4 \tag{4}$$

The Q-system for rock mass classification, developed at the Norwegian Geotechnical Institute (NGI) in 1974, (Barton et al. 1974). It is a quantitative classification system for estimates of tunnel support, based on a numerical assessment of the rock mass quality using the following six parameters: (a) RQD, (b) Number of joint sets (J_n), (c) Roughness of the most unfavourable joint or discontinuity (J_r), (d) Degree of alteration or filling along the weakest

Table 3 The RMR_{basic} and SMR of studied rock slope along Silchar-Haflong NH (loose debris cover was observed at Location L2, hence rockmass classification was not possible)

Parameters (with ratings)	Locations						
	L1	L3	L4	L5	L6	L7	L8
UCS (MPa)	65	59	66	47	65	58	68
rating	7	7	7	4	7	7	7
RQD (%)	78	38	63	10	58	65	48
rating	17	8	13	3	13	13	8
Mean discontinuity spacing (m)	5	0.25	0.5	0.02	0.38	0.6	0.34
rating	20	10	10	5	10	10	10
Discontinuity condition							
Persistence	< 1m	10–20 m	3–10 m	3–10 m	3–10 m	3–10 m	3–10 m
rating	6	1	2	2	2	2	2
Aperture	none	1–5 mm	0.1–1.0 mm	0.1–1.0 mm	< 0.1 mm	1–5 mm	0.1–1.0 mm
rating	6	1	4	4	5	1	4
Roughness	Very rough	Slightly rough	Slightly rough	Smooth	Slightly rough	Slightly rough	Smooth
rating	6	3	3	1	3	3	1
Infillings	Hard filling	Soft filling	Soft filling	Soft filling	Soft filling	Soft filling	Soft filling
rating	6	2	2	2	2	2	2
Weathering discontinuity surface	Moderately weathered	Moderately weathered	Moderately weathered	Moderately weathered	Moderately weathered	Moderately weathered	Moderately weathered
rating	3	3	3	3	3	3	3
Groundwater Condition	Dry	Dry	Dry	Dry	Dry	Dry	Dry
rating	15	15	15	15	15	15	15
RMR_{basic}	86	50	59	39	60	56	52
SMR	86	41	56	30	57	47	43
Q_{slope}	8.32	0.48	4.73	0.10	4.35	0.08	1.20
Existing slope angle	85°	80°	75°	80°	78°	70°	82°
Safe slope angle (Based on Q_{slope} stability chart)	Quasi-stable condition at 85°	59°	Already stable at 75°	45°	Stable to Quasi-stable condition at 78°	43°	67°

joint (J_a), (e) Water inflow (J_w), and, (f) Stress condition given as the stress reduction factor (SRF) (Eq. 5) (more details can be found in (Barton et al. 1974)).

$$Q = \frac{RQD}{J_n} \times \frac{J_r}{J_a} \times \frac{J_w}{SRF} \quad (5)$$

For the determination of optimal rock slope angle (β) of cut slopes along the studied road section, the Q_{slope} method was used which was first introduced by Barton and Bar (2015). This method is a modified version of Barton's Q system of rockmass classification (Barton et al. 1974). The Q_{slope} values were determined as per the suggested guidelines of Bar and Barton (2017) and plotted in Fig. 4. Numerous researchers have employed rock mass classification systems such as RMR, SMR, its extensions, GSI, and Q_{Slope} method to ascertain the prevailing slope stability conditions (Umrao et al. 2015; Siddique et al. 2017, 2020; Singh and Kumar 2020; Komadja

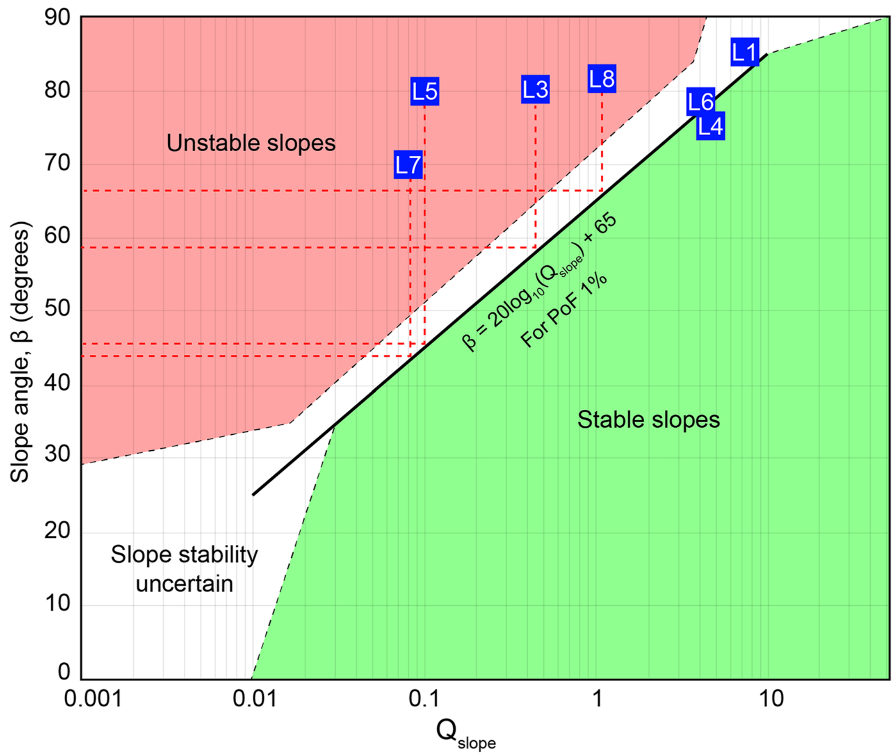

Fig. 4 Slope stability prediction chart based on Q_{Slope} values where the stable slope area is shown in green, unstable area is shown in red and the rest white area represents uncertain slope stability. The existing slope angles are colored in blue squares with location numbers and their projected stable slope angle (β) for probability of failure (PoF) of 1% (modified after (Bar and Barton 2017))

et al. 2021). Singh and Kumar (2020) conducted a detailed assessment of road cut slope stability along the Chamba-Bharmour Section (Chamba District, Himachal Pradesh) spanning from Chakki (Pathankot, Punjab) to Bharmour (Chamba, Himachal Pradesh). Rock mass characterization methodologies, RMR and modified SMR, were employed to assess instability and to identify potential failure slopes. Fourteen unstable slopes were evaluated for criticality using RMR and modified SMR methods, determining their stability classes.

3.3 Rainfall Characteristics

Climate change is causing great concern in the north-eastern section of India, which receives more rainfall than other parts of the subcontinent. Its impacts manifest in high-intensity rainfall for short durations and prolonged dry spells not just affect flood and drought situations but also the river morphology. On average the study area receives heavy rainfall during the monsoonal months particularly in June, July, August, and September (JJAS). Additionally, the presence of clay makes these rocks highly susceptible to intense weathering. Further, the presence of closely spaced bedding parallel joints allow rainwater to percolate deeper into the sedimentary formation (Singh et al. 2016a). The rainfall data of the study area from 1981 to 2022 suggest that the annual precipitation ranges between 1200 and 5000 mm (Fig. 5). More than 60% of the average rainfall occurs during monsoon months (Fig. 6). There is a drastic increase in the cumulative annual precipitation in the study area from 2014 onwards. This overall rainfall variability may be directly linked to climate change, which affects the intensity and frequency of precipitation throughout the region. The frequent heavy rainfall in these geologically young and steep mountains causes numerous slope failure events (Fig. 2), (Table 4).

Rainfall plays a significant role in causing instability in rock slopes, as most slope failures occur during the rainy season. When it rains, water flows down the upper slope and easily infiltrates tension cracks, contributing to the potential for slope failure. The instability is primarily influenced by the resistance to sliding along the potential failure surface, which is determined by shear strength parameters, specifically cohesion (c) and friction angle (φ). Percolating

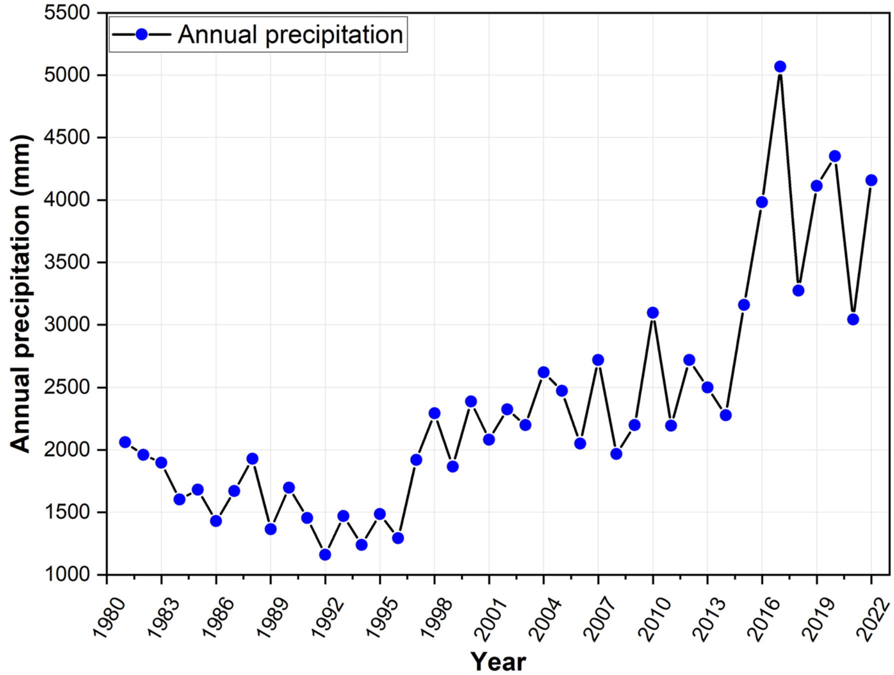

Fig. 5 Annual precipitation of the study area (Latitude: 24.9998 & Longitude: 92.7545) from 1981 to 2022

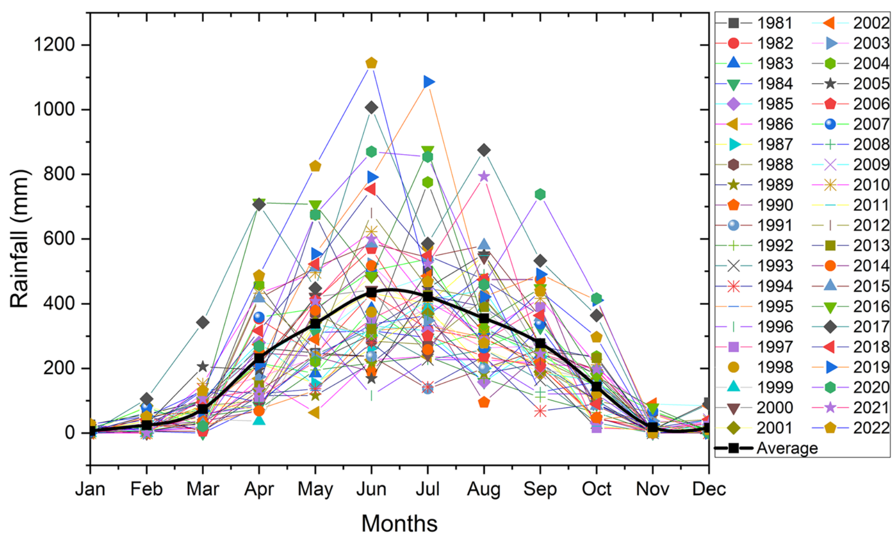

Fig. 6 Monthly rainfall data (in mm) of the study area

rainwater reduces these shear strength parameters along this potential failure surface (PFS). The PFS is contingent upon various other engineering geological characteristics of the discontinuity surface, including the surface's orientation, continuity, roughness, and aperture. Evaluating these characteristics is essential for understanding the shear strength of the potential failure surface, φ along this surface can be estimated using the principles of friction (Raghuvanshi 2019).

3.4 Methods for Slope Stability Assessment

3.4.1 Kinematic Analysis

The design of a stable slope requires the application of both empirical and numerical methods. Many studies use the RMR, SMR, and Q_{slope} rock mass categorization schemes, which have acquired universal recognition. However, these approaches

Table 4 Few recent major slope failures along the Silchar-Haflong-Lumding NH. (Source: Barak Bulletin (2023), Times of India (2022), Deccan Herald (2020), Pratidin Time (2019), Northeast Now (2018), Business Standard (2016))

Event date	Type/location	Effects/casualties
28 May 2024	Severe landslides in Kapircherrra and ThereBasati, in Assam's Dima Hasao district	Landslides have severely impacted NH-27, particularly the Haflong-Silchar Link Road and the Umrangso-Dehangi Road. Continuous downpours have eroded large sections of these roads, worsening disruptions. Rising river levels have further complicated navigation for vehicles
02 May 2024	Landslides in Jatinga-Lampur and New Harangajao stations in Dima Hasao district	Transportation and critical services are disrupted, presenting significant challenges for the region. The landslides have necessitated the suspension of the Lumding-Silchar rail service, while torrential rains have intermittently impeded communication with Haflong by rendering the railway route at Maibang inoperable
11 June 2023	Balacherra portion of the Silchar-Haflong NH located in the Cachar district	The landslide disrupted traffic in the area as hundreds of vehicles from both sides got stranded
14 May 2022	Silchar-Haflong highway closed to traffic after landslides	Landslides impacted surface communication on several routes, including the Haflong-Dehangi and New Haflong-Jorai-Michidui highways in the hill area. Minor landslips have occurred in many regions around Haflonq, Dima Hasao's headquarters
24 March 2022	Heavy landslide at Silchar-Haflong NH	Landslide closes Silchar-Haflong NH caused by torrential rains. The highway has been closed for landslides causing considerable inconvenience to commuters
2 June 2020	Shallow translational Landslide at Kanakpur Pt. III, Lakhipur, Joypur	The Kanakpur landslide claimed lives of 7 people and 1 person was injured. The house was completely buried under the slide material destroying one tin-roofed kaccha house
9 November 2019	Heavy landslide at Lumding NH-27	Horrific landslides have been taken place in the Lumding-Myanmar connecting NH-27 due to rainfall for several days. Due to the landslide, one side of the 4-lane has completely eroded leading to deadly accidents
27 October 2019	Disrupted rainfall causes landslide in Dima Hasao	The landslide damaged houses and roads in many parts of the district mainly in Maibang, Mahur, Langting, Hatikhali, and Harangajao region and the Haflong-Silchar road was cut off completely due to heavy rainfall and landslide at various places. In Hatikhali the Hatikhali police outpost was also flooded with rainwater
14 June 2018	Multiple landslides at six places in the Dima Hasao district	Constant rainfall caused large landslides in six locations between New Haflong and Lumding, including Mupa, Daotuhaja, and Phaiding, disrupting road and railway connectivity in the district
3 April 2017	Landslides at Barail hills, Kapurcherra near Harangajao in Dima Hasao district	The NH-54 (East), linking Silchar and Haflong, experienced a 12-day closure. Subrata Paul (48), a school teacher from the hilly district, was traversing a section of the Haflong-Silchar road on foot near Kapurcherra, close to Harangajao when he was swept away by a deluge of rainwater cascading from the Barail hills

Table 4 (continued)

Event date	Type/location	Effects/casualties
16 May 2016	Multiple landslides at several places, in Dima Hasao district	Heavy rain and consecutive landslides over two days resulted in complete isolation of Haflong by road, with train services being suspended on various routes. The primary road linking Haflong was affected at multiple points, causing temporary blockages on DD Road, NH 54, along the Haflong-Lumding and Haflong-Silchar routes
26 June 2012	landslide in Mahadevtila locality, three km from Haflong, Dima Hasao district	Claimed the lives of two women. Four others, including one woman, were injured
4 June 2012	Multiple Landslides along the Lumding-Silchar section of Northeast Frontier Rail (NFR)	The landslide results from several days of heavy rain in the Barail Hill range. A considerable amount of debris washed down Barail Hill on the railway tracks at five different locations in the Dima Hasao area, causing a 130-m stretch to be washed away
23 May 2011	Landslide at Reko near Harangajao in Dima Hasao district	The 110-km Silchar-Haflong road is closed for 18 days. The mudslide wiped away a 200-m piece of road. A freight train derailed between Harangajao and Mailongdisa, resulting in the cancellation of all trains in that stretch
24 April 2010	Landslides triggered by heavy rainfall at four locations in the Lumding-Silchar	Several trains were canceled or short-terminate a few trains

cannot provide a slope's stress distributions and failure characteristics (Kainthola et al. 2012). Since most landslide studies have been motivated by an applied viewpoint, slope stability analysis and hazard prediction have been prominent research focus.

Block failure analysis was conducted utilizing the "Dips" computer software, specifically designed for the graphical and statistical evaluation of orientation-related geological data. This software assesses the direction in which blocks may slide and deduces their stability status. This process is commonly referred to as kinematics analysis. The purpose of this method is to assess the likelihood of different types of rock slope failures (including plane, wedge, and toppling failures) resulting from unfavorable orientations of geological features like joints, faults, bedding planes, foliation, and shear zones, which could potentially act as planes of failure (Yoon et al. 2002; Das and Singh 2021). The kinematic method deals with the failure mode of the rock slope without reference to the forces that cause them to move (Goodman 1989; Lamessa and Meten 2021).

3.4.2 Numerical Modelling

A 2D finite element method (FEM) based program named *Phase*^{2} (Rocscience Inc. 2016) was used to model the rockmass and access the slope stability condition. The model includes initial model setup, mesh generation, boundary conditions, field stress, and simulation. Three-node triangular planar elements were utilized to mesh the problem domain to simulate the rockmass because they are easy to create and can handle uneven boundaries (Carroll 1998; Das et al. 2017). Graded mesh types were used, with a gradation factor of 0.1. Fixed restraints were applied to the sides and bottom of the model (i.e. no movement in X and Y directions), while the top ground surface was left free. For the simulation, gravity field stress option is selected to provide an in-situ stress field that changes with depth. Gravity field stress is commonly employed for surface or near-surface excavations.

The numerical model illustrates a plane strain analysis in which the strain in the out-of-plane direction is zero. The rockmass is modeled as a elastoplastic material with a Mohr–Coulomb yield condition (Eq. (6)).

$$\tau = \sigma_n \tan \phi + c \tag{6}$$

where σ_n is the normal stress, τ is shear stress, ϕ is internal friction angle, and c represents cohesion. The shear strength reduction (SSR) technique is applied to determine the Factor of safety (FoS) because in FEM analysis, tracing the failure slip surface of a slope presents a formidable challenge due to its reliance on the stress-based failure criterion (Matsui and San 1992). Komadja et al. (2021) conducted a comprehensive geotechnical and geological investigation of the stability conditions of eight road cut debris-slopes along NH-7 in Uttarakhand, India. The stability conditions were evaluated using both deterministic and probabilistic limit equilibrium slope stability approaches. The reliability of the analyses was benchmarked against the Finite Element Method (FEM) utilizing the SSR technique. Laboratory experiment conducted by Roscoe (1970) showed that the failure shear strain zone coincided with the rupture surface. This leads to the supposition that the slope's failure mechanism is intricately linked to the evolution of shear strain within the SSR technique where the general assumption is that strain relies on shear strength. Because slope stability hinges on its shear strength, as the shear strength diminishes, the strain within the slope intensifies, indicating the potential area of failure. The relationship between shear strength and strain in a hyperbolic stress and strain model as presented by Duncan and Chang (1970), (Eq. (7)):

$$\varepsilon = \frac{\sigma_1 - \sigma_3}{E_i\left[1 - \frac{R_f(\sigma_1-\sigma_3)(1-\sin\phi_r)}{(2c_r\cos\phi_r + 2\sigma_3\sin\phi_r)}\right]} \tag{7}$$

where ε is the axial strain, σ_1 and σ_3 are the major and minor principal stress, E_i the initial tangent modulus, R_f the failure ratio, c_r and ϕ_r are the reduced shear strength parameters, defined as (Eq. (8)).

$$c_r = \frac{c}{R}, \quad \tan\phi_r = \frac{\phi}{R} \tag{8}$$

Where, c and ϕ are the shear strength parameters, and R the shear strength reduction factor (SRF), i.e. simulations will be run for a series of trial factors of safety R with c and ϕ adjusted until the slope fails.

To model the joints, the Barton-Bandis joint slip criterion is used (Barton 1973, 1976; Barton and Choubey 1977), (Eq. (9))

$$\tau_j = \sigma_n \tan\left[\phi_{rf} + JRC\log_{10}\left(\frac{JCS}{\sigma_n}\right)\right] \tag{9}$$

where τ_j is the shear strength of joint (MPa), σ_n is the normal stress (MPa), JCS is the joint wall compressive strength (MPa), JRC is the joint wall roughness coefficient (unitless), and ϕ_{rf} represents the residual friction angle (in degree). The joints are modeled assuming a linear elastic behavior and thus the influencing parameters on the joint behavior are joint's normal stiffness (K_n) in MPa/m and shear stiffness (K_s) in MPa/m, (Eq. (10)) i.e.

$$K_n = \frac{\sigma_n}{v_j}, \qquad K_s = \frac{\tau_j}{d_h} \tag{10}$$

where, v_j is the normal displacement (m), and d_h is the shear displacement (m).

The input parameters for the rocks were determined in the laboratory and their petrographic characteristics were party taken from published literature (Bharali et al. 2017; Borgohain et al. 2020) (Table 6). Borgohain et al. (2020) reported that the Oligocene Barail Sandstones of Surma basin are poor to moderately sorted, subarkosic to sub-litharenite and show dominance of quartz 54.46% followed by feldspars 7.22%, rock fragments 4.98%, mica 5.89%, matrix 14.47% and cement 12.98%. It is moderately mature, grayish to reddish color and experienced medium to high intensity of chemical weathering in the parent rocks under humid climatic condition. Bharali et al. (2017) studied the characteristics of Upper Bhuban sandstones and are found to be medium to fine grained, massive and moderately to well sorted. Quartz grains were dominant and are the most common detrital constituents constituting an average of 43.28% of the total framework grains. Lithic fragments were also found at 7.50%, feldspars 5.71%, and micas 9.82%. Quartzs are sub-angular to sub-rounded in shape and are generally monocrystalline in nature, but polycrystalline varieties are also found.

3.4.3 Rockfall Analysis

The relative movement of a falling boulder down a slope may depend on various factors: lithology, topography, slope inclination, the size and shape of the boulder, number and frequency of discontinuities on the outcrop and the extent of weathering along the plane of vulnerability (Schweigl et al. 2003; Singh et al. 2013). In the present study, the 2D simulation of the fall of boulders was performed using the "Rockfall" computer program. The simulation is performed using the statistical analysis of rockfall based on a "lumped-mass" method to forecast the trajectory of falling rocks and estimate the energy loss they experience during their descent. This technique considers the boulder's mass to be a single point travelling through the air on a ballistic trajectory. When the falling block encounters the slope, the normal and tangential components of speed change depending on the coefficients of reaction and resistance of the soils along the rockfall's trajectory. The reaction coefficients are supposed to be overall values that consider all aspects of impact, such as deformation, sliding upon contact, and the conversion of rotational moments into translational moments, and vice versa. The initial conditions used in the rockfall simulation is tabulated in Table 5.

4 Results and Discussion

4.1 Kinematic Analysis of Critical Slopes

The initial investigation into slope stability primarily centers on analyzing how discontinuities behave under field conditions. It is crucial to articulate the likelihood of a rock slope failing when characterizing the rock mass. To accurately forecast the behavior of the rock slope, it's important to establish the orientations of the relationships between slope discontinuities that are compatible with the rock mass. Introduced by Markland (1972), this technique is straightforward and user-friendly, employing a stereonet to assess the feasibility of failure. In our current study, we utilized Dips 6.0 (Rocscience 2015) a widely-used software designed to effectively predict various types of failures (such as Wedge, Planar, and Toppling). A wedge failure occurs in a slope when two or more discontinuities form a line of intersection that plunges at an angle less steep than the slope inclination but steeper than the internal frictional angle of the rock material. Planar failure, on the other hand, involves a joint plane aligned similarly to the slope face but with a lower dip than the slope itself and a higher dip than the frictional angle. Toppling failure is most prevalent in steeply inward-dipping slopes and occurs when the rock mass's center of gravity moves beyond the slope's boundaries.

The selected area for kinematic analysis comprises four locations: L3, L5, L7, and L8. L3 is characterized by sandstone, which is both fragile and weak, as depicted in (Fig. 7a). The primary joint, J1, has a dip of 76° toward 182°, while the sandstone's friction angle is 30°. Planar failure along the highway significantly impacts this site. Moving on to L5, it primarily consists of siltstone, as shown in Fig. 7b. This slope features two major joints: J1, which is nearly horizontal with a dip of 36° at 270°, and J2, a vulnerable joint oriented at 321° with a dip of 72°. The analysis indicates a high likelihood of planar failure occurring along J2 in this slope.

Site L7 has three sets of joints, each exhibiting distinct characteristics. J1 lies moderately inclined, while J2 and J3 are steeply inclined (Fig. 7c). The sandstone at this location has a frictional angle of 27°. Based on kinematic analysis, it is evident that all three joints contribute to a wedge-type failure mechanism, with the potential failure zone spanning from 229° to 252°. This site is particularly susceptible to rockfalls, and recent incidents have been documented in Fig. 3g. Moving to location L8, we encounter another sandstone rock slope, as illustrated in Fig. 7d. Here, there are two sets of steeply

Table 5 Initial conditions used in the rockfall simulation

Parameter	Inputs
Slope material	Talus cover
Coefficient of normal restitution (R_n)	0.32 ± 0.04
Coefficient of tangential restitution (R_t)	0.82 ± 0.04
Friction angle (in degree)	30 ± 2
Analysis method	Lumped mass statistical analysis method
Numbers of block to throw	50
Mass of each rigid rock body	30 kg
Minimum velocity cut-off	0.1 m/sec
Rock density	2100 kg/m^3

Fig. 7 Field situation and Schmidt net plot (kinematic analysis of slope) of major discontinuities observed along the cut slopes **a** L3, **b** L5, **c** L7 and **d** L8

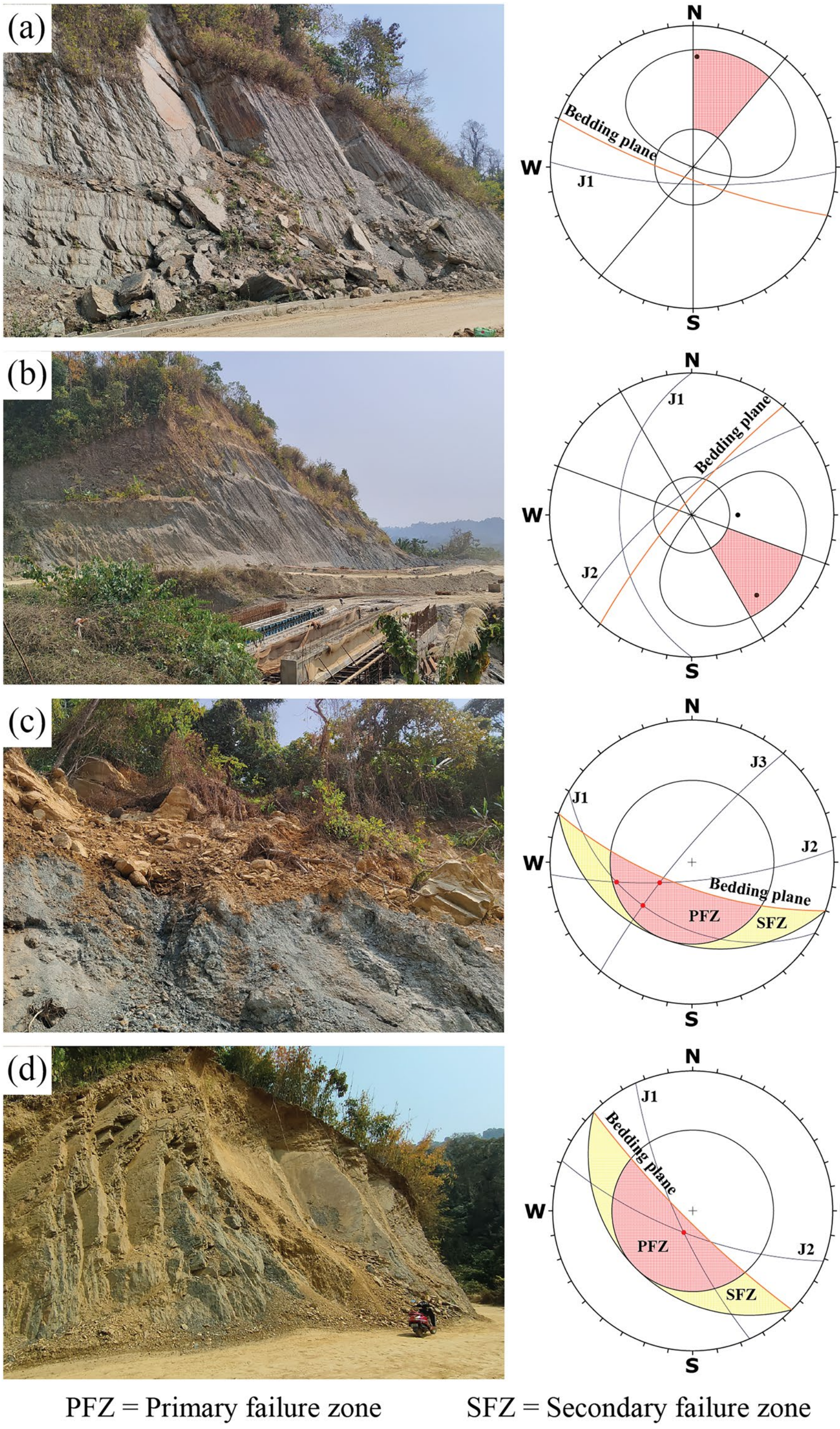

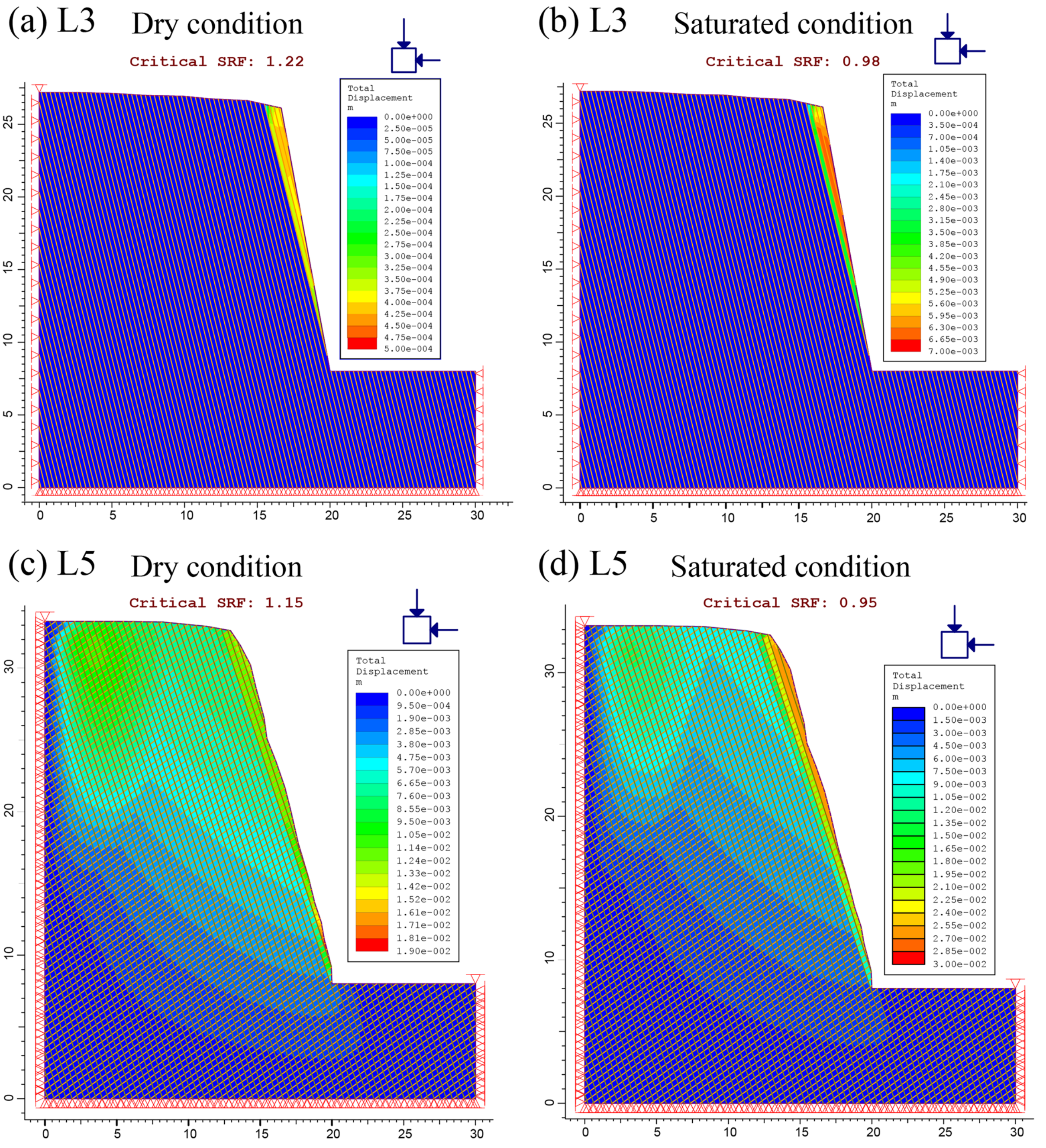

Fig. 8 Total displacement values, **a** Dry condition L3, and **b** Wet condition L3, **c** Dry condition L5, and **d** Wet condition L5

inclined joints that interact to create conditions conducive to wedge failure. Specifically, J1, with an orientation of 76° along 246°, and J2, at 71° along 201°, combine to form a vulnerable joint-slope orientation of approximately 202°.

Table 6 Average physico-mechanical properties of material as input parameters for the dry and saturated condition (L3, L5 and L8)

Material		Unit weight (MN/m^3)	Young's moduls (GPa)	Poisson's ration	Tensile strength (MPa)	Friction angle (°)	Cohesion, (*c*) (MPa)
Bhuban Sandstone (L3)	Dry	0.026	18	0.28	7.62	38	10
	Saturated	0.029	14	0.31	2.98	34	9
Bhuban shale (L5)	Dry	0.021	9	0.38	3.52	32	6
	Saturated	0.023	6	0.40	1.55	30	3
Barail sandstoe (L8)	Dry	0.026	19	0.27	8.23	36	9
	Saturated	0.028	15	0.30	3.02	33	7

4.2 Numerical Results

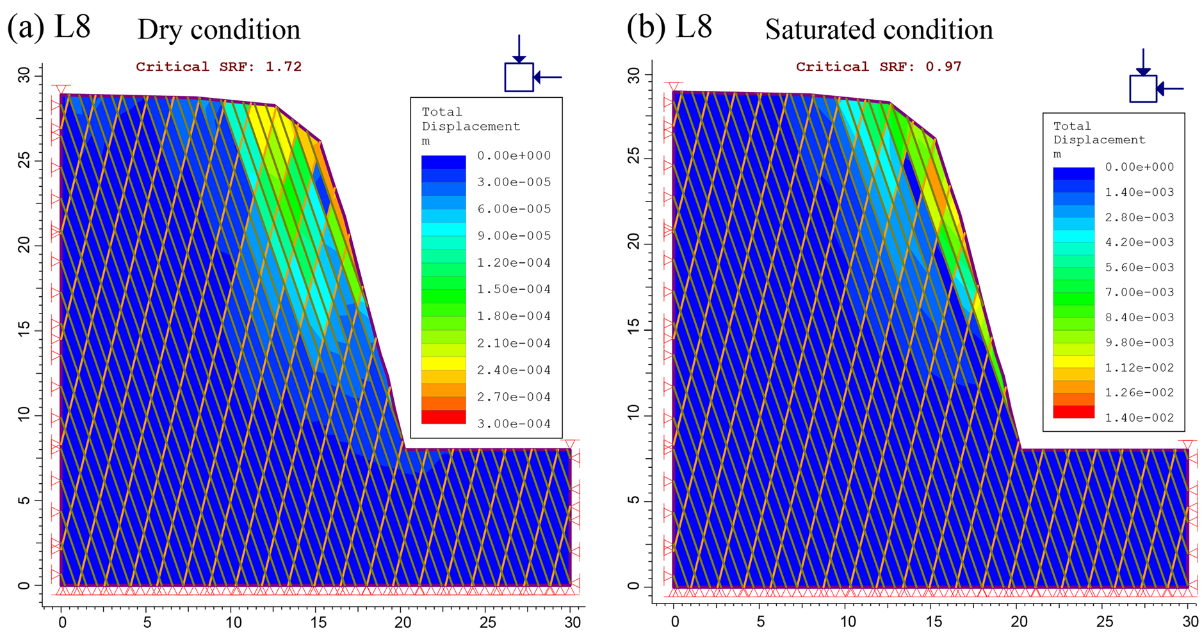

Fig. 9 Total displacement values, **a** Dry condition L8, and **b** Saturated condition L8

Table 7 Model input parameters for joints

Joint parameters		JCS (MPa)	JRC	Residual friction angle, ϕ_{rf} (°)	Normal stiffness, K_n (MPa/m)	Normal stiffness, K_s (MPa/m)
L3	Joint (dry)	59	3	35	10,000	1000
	Joints (saturated)	59	3	25	1000	100
L5	Joint (dry)	47	6	30	10,000	1000
	Joints (saturated)	38	6	28	1000	100
L8	Joint (dry)	47	6	30	10,000	1000
	Joints (saturated)	42	6	28	1000	100

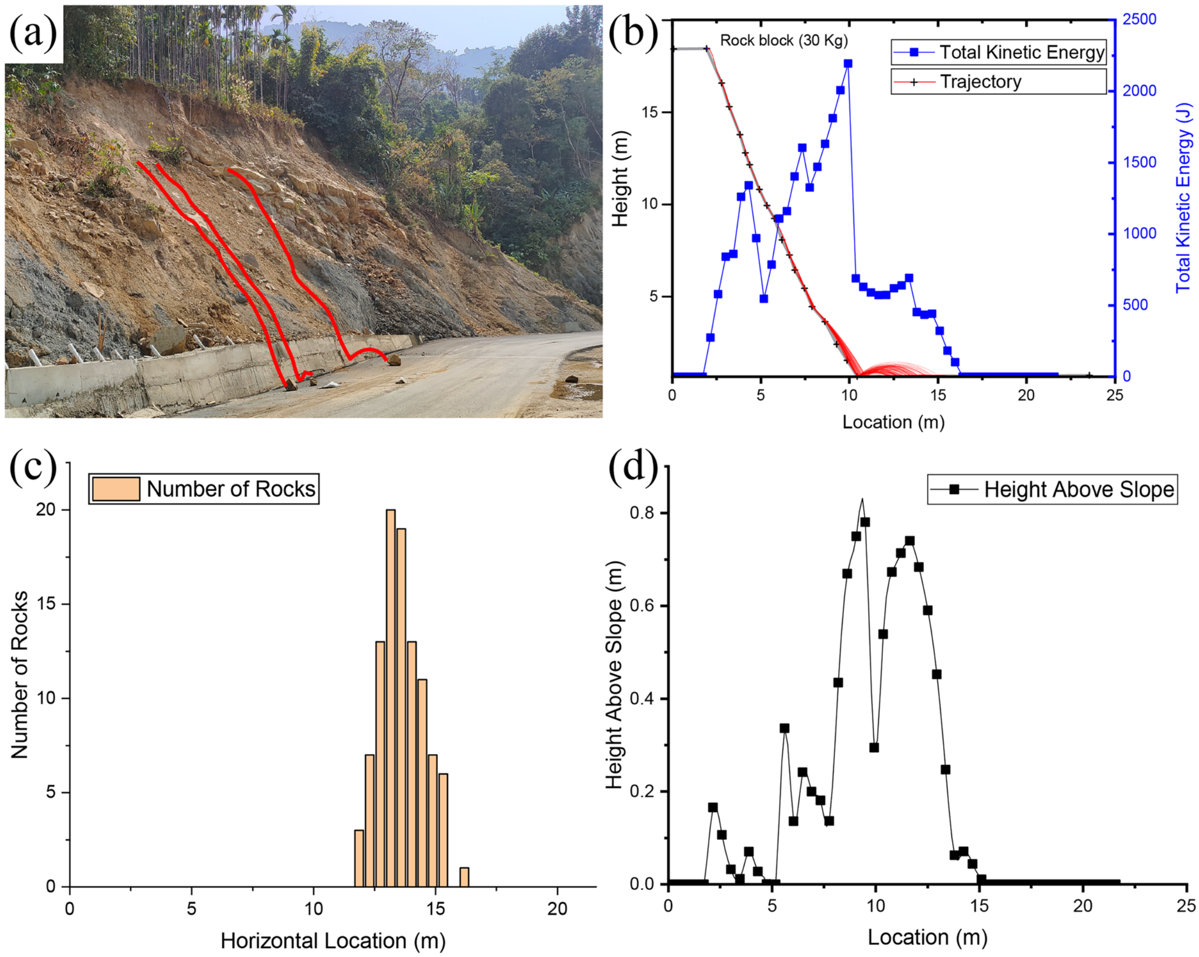

Fig. 10 Rockfall simulation results for location L7 slope profile **a** actual rockfall site (L7), **b** rockfall profile-throw trajectories, fifty movement paths were calculated for rock block of mass 30 kg, and a total kinetic energy (in Joule) distribution was obtained, **c** Horizontal location of rock endpoints and **d** Studied section showing rockfall bounce height versus distance traveled

The results of the finite element model are presented in Figs. 8 and 9. The critical slopes (L3, L5 and L8) were simulated with finite element modeling (FEM) using *Phase*^{2} software under both dry and saturated condition to determine the corresponding critical strength reduction factor (SRF). It is almost impossible for any slope to be totally dry. Therefore, in this study, we determined the physico-mechanical properties of the in-situ rock samples. The term "Dry condition" basically imply the rock condition in its natural moisture content during non-monsoon period. In the FEM analysis result, the word "saturated" means that we improvised our material model in such a way that the rock material behaves as fully saturated rock material. This was achieved by reducing the mechanical parameters to saturated condition (Tables 6 and 7). For dry condition, the critical SRF values observed for L3, L5 and L8 were 1.22, 1.15 and 1.72, respectively. Whereas for saturated condition the critical SRF values were 0.98, 0.95 and 0.97 for location L3, L5 and L8, respectively. Plane failure occurred within the stratified sedimentary rocks as the bedding planes were exposed on the excavated road cut slope at an angle less steep than the slope itself. In all three locations, the primary internal governing factors such as slope geometry and characteristics of the potential failure plane, favored the occurrence of a slide. These conditions were further exacerbated by external factors, specifically rainfall and human activities associated with construction on unscientific cut slopes.

4.2.1 Rockfall Analysis Results of Problematic Slope (L7)

At location L7, rock blocks are formed due to the presence of critically oriented joint planes which create avenues for the initiation of rockfall. As discussed earlier, most rockfall occurs due to the detachment of blocks by either planar or wedge failure mode (Ahmad et al. 2013). Therefore, joint data was used to determine mode of failure using kinematic analysis (Fig. 7c). Also, the slope material appeared highly weathered due to heavy rainfall, significantly reducing the strength of joint. The rockfall analysis provide results in terms of quantities like bounce heights, kinetic energy translational velocity and travel distance (Fig. 10). Ritchie (1963) suggested that the falling blocks attain different types of motion depending upon the slope geometry and mechanical characteristics of the blocks. Ahmad et al. (2013) observed that the slope geometry, exerts a more significant influence on rockfall dynamics compared to the mass of the rock block. During the rockfall, the motion like rolling, sliding and bouncing, the falling mass continuously interacts with the surface and changes their direction and energy with each impact (Dorren 2003). As the rock block descends, initially the KE increases but eventually it loses its KE and become stationary (Fig. 10b). There are various factors due to which this loss in the KE is observed, during the collision of the rock block with contact surface. The KE gets converted in sound energy, frictional energy, thermal energy etc. But in general, during the calculation of rockfall impact forces using elastic-plastic contact theory, the frictional energy dissipation between the rockfall and the object it contacts is usually overlooked (Chen et al. 2023). In reality, rockfall impacts are dynamic events where contact damping plays a role in dissipating a portion of the impact energy.

The falling block trajectory and the energy distribution of the rockfall is shown in Fig. 10a,b. When falling block collides with the slope or the contact surface, kinetic energy loss occurs (Singh et al. 2016b; He et al. 2021). Some small fluctuations in the energy distribution correspond to the bounce of the rockfall movement in the trajectory. The trajectory of the falling block show that the blocks are capable enough to reach the roadways and end their journey in the middle of the highway, which may be very dangerous for the commuters or element at risk (Fig. 10a).

4.3 Limitations

In the current study, our primary focus was understanding slope failure mechanisms under static conditions, specifically those driven by material properties, saturation conditions, and surface loading. Our objective was to establish a baseline understanding of slope stability in the absence of dynamic forces, which is critical for accurately isolating the effects of these factors. However, we acknowledge the importance of considering dynamic forces, such as seismic activity, in comprehensive slope stability analyses. Earthquakes and other dynamic events can significantly influence slope stability, and their exclusion may limit the scope of our findings.

5 Conclusion

The study focuses on the geotechnical insights of the cut slopes situated in a vulnerable geological setting along Silchar-Haflong National Highway, Assam, India, revealing a history of more than 158 slope failures. This was done using different rock mass classification techniques including detailed field observation. Detailed engineering geological investigations were conducted on a specific 25 km section along the route where the region's complex geological and geotechnical conditions led to potentially unstable cut slopes. Various rock mass characterization methods, including RMR_{basic}, SMR, and Q_{slope}, were employed to characterize the slope mass condition. Data from 1981 to 2022 reveal a significant increase in cumulative annual precipitation since 2014 in the study area. The frequent heavy rainfall, combined with the geological characteristics of the young and steep mountains, contributes to numerous slope failure events, mainly occurring during the monsoon season. Kinematic analysis identified four unstable locations (L3, L5, L7, and L8) in heavily jointed rock masses. The findings reveal that the slope geometry and characteristics of the potential failure plane favor planar sliding (L3, L5, and L8), especially when exacerbated by external factors like rainfall and construction activities. FEM was employed to determine critical SRF for dry and saturated conditions in the critical slopes at L3, L5, and L8. For dry conditions, the critical SRF values observed for L3, L5 and L8 were 1.22, 1.15 and 1.72, respectively. Whereas for saturated condition the critical SRF values were 0.98, 0.95 and 0.97 for location L3, L5 and L8, respectively. The study delves into rockfall analysis for a problematic slope (L7) and highlights the critical role of oriented joint planes in prompting rockfall events. The rockfall analysis provides results in quantities like bounce heights, kinetic energy translational velocity, and travel distance. The trajectory of the falling block shows that the blocks are capable enough to reach the roadways and end their journey in the middle of the highway, which may be very dangerous for the commuters or element at risk. The research findings have practical implications for slope stability assessment, rockfall hazard mitigation, and the safety of infrastructure and commuters.

Acknowledgements The first author would like to thank and acknowledge the financial support provided by Science and Engineering Research Board (SERB), a statutory body of the Department of Science and Technology (DST), Government of India under the Start-up Research Grant (SRG) scheme File Number: SRG/2022/000447. The author thankfully acknowledges the NASA and Bhukosh (Govt. of India) portals for their freely available data. We also wish to acknowledge the outstanding editorial handling by the editor-in-chief, Mohamed A. Meguid. We are also grateful for the constructive comments and valuable suggestions from the anonymous reviewers and the editor on an earlier draft, which helped clarify certain points and improve the overall quality of the manuscript.

Author contributions **Ratan Das**: conceptualization, fieldwork, writing—original draft, review and editing, resources, data preparation and data processing, formal analysis, software, experimental tests and numerical simulation, visualization, interpretation. **T N Singh**: supervision, Writing—review and editing, formal analysis, resource.

Funding DST-SERB, Government of India, supported this work.

Data availability The dataset is included in the manuscript.

Declarations

Conflict of interests The author declares that they have no conflict of interests.

References

Ahmad M, Umrao RK, Ansari MK et al (2013) Assessment of rockfall hazard along the road cut slopes of State Highway-72, Maharashtra, India. Geomaterials 03:15–23. https://doi.org/10.4236/gm.2013.31002

Alam Laskar A, Phukon P (2013) Structural control on landscape development of Barak Valley, Northeast India. J Geol Soc India 81:232–240. https://doi.org/10.1007/s12594-013-0026-6

ASTM D7012-23 (2023) Standard test methods for compressive strength and elastic moduli of intact rock core specimens under varying states of stress and temperatures. ASTM Int West Conshohocken, PA, United States. https://doi.org/10.1520/D7012-23.1.5.1.1

Bar N, Barton N (2017) The Q-slope method for rock slope engineering. Rock Mech Rock Eng 50:3307–3322. https://doi.org/10.1007/s00603-017-1305-0

Barton N (1973) Review of a new shear-strength criterion for rock joints. Eng Geol 7:287–332. https://doi.org/10.1016/0013-7952(73)90013-6

Barton N (1976) The shear strength of rock and rock joints. Int J Rock Mech Min Sci Geomech Abstr 13:255–279. https://doi.org/10.1016/0148-9062(76)90003-6

Barton N, Choubey V (1977) The shear strength of rock joints in theory and practice. Rock Mech 10:1–54. https://doi.org/10.1007/BF01261801

Barton N, Lien R, Lunde J (1974) Engineering classification of rock masses for the design of tunnel support. Rock Mech 6:189–236. https://doi.org/10.1007/BF01239496

Barton N, Bar N (2015) Introducing the Q-slope method and its intended use within civil and mining engineering projects. In: Schubert W, Kluckner A (Eds) Future development of rock mechanics: Proceedings of the ISRM regional symposium, Eurock 2015 and 64th geomechanics colloquium. Salzburg, Austria, pp 157–162

Bera A, Mukhopadhyay BP, Das D (2019) Landslide hazard zonation mapping using multi-criteria analysis with the help of GIS techniques: a case study from Eastern Himalayas, Namchi, South Sikkim. Nat Hazards 96:935–959. https://doi.org/10.1007/s11069-019-03580-w

Bharali B, Borgohain P, Bezbaruah D et al (2017) A geological study on Upper Bhuban formation in parts of Surma Basin, Aizawl, Mizoram. Sci vis 17:128–147

Bieniawski ZT (1989) Engineering rock mass classifications: a complete manual for engineers and geologists in mining, civil, and petroleum engineering, 1st edn. John Wiley & Sons-Interscience, New York

Borgohain P, Hussain MF, Bezbaruah D et al (2020) Petrography and whole-rock geochemistry of Oligocene Barail sandstones of Surma basin: implications for tectono-provenance and paleoclimatic condition. J Earth Syst Sci 129:179. https://doi.org/10.1007/s12040-020-01431-y

Carroll WF (1998) A Primer for finite elements in elastic structures. John Wiley & Sons Inc

Chen T, Zhang G, Xiang X (2023) Research on rockfall impact process based on viscoelastic contact theory. Int J Impact Eng 173:104431. https://doi.org/10.1016/j.ijimpeng.2022.104431

Crosta GB, Frattini P (2008) Rainfall-induced landslides and debris flows. Hydrol Process 22:473–477. https://doi.org/10.1002/hyp.6885
Das R, Singh TN (2021) Effect of closely spaced, non-persistent ubiquitous joint on tunnel boundary deformation: a case study from Himachal Himalaya. Geotech Geol Eng 39:2447–2459. https://doi.org/10.1007/s10706-020-01637-3
Das R, Singh PK, Kainthola A et al (2017) Numerical analysis of surface subsidence in asymmetric parallel highway tunnels. J Rock Mech Geotech Eng 9:170–179. https://doi.org/10.1016/j.jrmge.2016.11.009
Das R, Phukon P, Singh TN (2022) Understanding the cause and effect relationship of debris slides in Papum Pare district, Arunachal Himalaya, India. Nat Hazards 110:1735–1760. https://doi.org/10.1007/s11069-021-05010-2
Deere DU (1964) Technical description of rock cores for engineering purposes. Rock Mech Eng Geol 1:16–22
Dhar ON, Nandargi S (2004) Rainfall distribution over the Arunachal Pradesh Himalayas. Weather 59:155–157. https://doi.org/10.1256/wea.87.03
Dorren LKA (2003) A review of rockfall mechanics and modelling approaches. Prog Phys Geogr Earth Environ 27:69–87. https://doi.org/10.1191/0309133303pp359ra
Duncan JM, Chang C-Y (1970) Nonlinear analysis of stress and strain in soils. J Soil Mech Found Div 96:1629–1653. https://doi.org/10.1061/JSFEAQ.0001458
Fang H, Cui P, Pei LZ, Zhou XJ (2012) Model testing on rainfall-induced landslide of loose soil in Wenchuan earthquake region. Nat Hazards Earth Syst Sci 12:527–533. https://doi.org/10.5194/nhess-12-527-2012
Ganguly S (1983) Geology and hydrocarbon prospects of Tripura-Cachar-Mizoram region. Pet Asia Jour 6:105–109
Ganguly S (1984) Tectonic evolution of the orogenic belt of Tripura. Q J Geol Mining Metall Soc India 56:128–137
Gipprich TL, Snieder RK, Jibson RW, Kimman W (2008) The role of shear and tensile failure in dynamically triggered landslides. Geophys J Int 172:770–778. https://doi.org/10.1111/j.1365-246X.2007.03681.x
Goodman RE (1989) Introduction to Rock Mechanics, Second. John Wiley & Sones
GSI (2019) Geology and mineral resources of assam, geological survey of India, miscellaneous publication, No. 30, Part 4, Vol. 2 (i), Third Ed. Director General, Geological Survey of India
Guhathakurta P, Khedikar S, Menon P, et al (2020) Climate Research and Services Observed Rainfall Variability and Changes over Assam State. IMD Annu Rep 28
Guzzetti F, Peruccacci S, Rossi M, Stark CP (2008) The rainfall intensity-duration control of shallow landslides and debris flows: an update. Landslides 5:3–17. https://doi.org/10.1007/s10346-007-0112-1
He Y, Nie L, Lv Y et al (2021) The study of rockfall trajectory and kinetic energy distribution based on numerical simulations. Nat Hazards 106:213–233. https://doi.org/10.1007/s11069-020-04457-z
Hungr O, Evans SG, Hazzard J (1999) Magnitude and frequency of rock falls and rock slides along the main transportation corridors of Southwestern British Columbia. Can Geotech J 36:224–238. https://doi.org/10.1139/t98-106
Rocscience Inc. (2016) Phase2 v.8, 2D Finite Element Software, Available from www.rocscience.com
Iverson RM (2000) Landslide triggering by rain infiltration. Water Resour Res 36:1897–1910. https://doi.org/10.1029/2000WR900090
Jaiswal A, Verma AK, Singh TN (2023) Evaluation of slope stability through rock mass classification and kinematic analysis of some major slopes along NH-1A from Ramban to Banihal, North Western Himalayas. J Rock Mech Geotech Eng. https://doi.org/10.1016/j.jrmge.2023.02.021
Kainthola A, Singh PK, Wasnik AB et al (2012) Finite element analysis of road cut slopes using Hoek and Brown. Int J Earth Sci Eng 5:1100–1109
Kanungo DP, Sharma S (2014) Rainfall thresholds for prediction of shallow landslides around Chamoli-Joshimath region, Garhwal Himalayas, India. Landslides 11:629–638. https://doi.org/10.1007/s10346-013-0438-9
Komadja GC, Pradhan SP, Oluwasegun AD et al (2021) Geotechnical and geological investigation of slope stability of a section of road cut debris-slopes along NH-7, Uttarakhand. India Results Eng 10:100227. https://doi.org/10.1016/j.rineng.2021.100227
Korup O (2005) Large landslides and their effect on sediment flux in South Westland, New Zealand. Earth Surf Process Landforms 30:305–323. https://doi.org/10.1002/esp.1143
Lamessa G, Meten M (2021) Stability analysis of rock slope along selected road sections from Gutane Migiru town to Fincha sugar factory, Oromiya, Ethiopia. SN Appl Sci 3:1–16. https://doi.org/10.1007/s42452-020-04026-w
Lee SG, Hencher SR (2009) The repeated failure of a cut-slope despite continuous reassessment and remedial works. Eng Geol 107:16–41. https://doi.org/10.1016/j.enggeo.2009.03.011
Loche M, Scaringi G, Yunus AP et al (2022) Surface temperature controls the pattern of post-earthquake landslide activity. Sci Rep 12:1–11. https://doi.org/10.1038/s41598-022-04992-8
Markland JT (1972) A useful technique for estimating the stability of rock slopes when the rigid wedge slide type of failure is expected. Interdepartmental Rock Mechanics Project, Imperial College of Science and Technology
Matsui T, San K-C (1992) finite element slope stability analysis by shear strength reduction technique. Soils Found 32:59–70. https://doi.org/10.3208/sandf1972.32.59
Mesri G, Huvaj-Sarihan N (2012) Residual shear strength measured by laboratory tests and mobilized in landslides. J Geotech Geoenvironmental Eng 138:585–593. https://doi.org/10.1061/(asce)gt.1943-5606.0000624
Mesri G, Shahien M (2003) Residual shear strength mobilized in first-time slope failures. J Geotech Geoenvironmental Eng 129:12–31. https://doi.org/10.1061/(asce)1090-0241(2003)129:1(12)
Nandy DR (2001) Geodynamics of the Northeastern India and the adjoining Region. ACB Publ 1–289
Paniagua P, L'Heureux JS, Grøneng G, et al (2021) Transport infrastructure and geotechnical engineering: ELGIP position paper. In: IOP Conference Series: Earth and Environmental Science p 012069
Pinyol NM, Alvarado M, Alonso EE, Zabala F (2018) Thermal effects in landslide mobility. Geotechnique 68:528–545. https://doi.org/10.1680/jgeot.17.P.054

Raghuvanshi TK (2019) Plane failure in rock slopes–a review on stability analysis techniques. J King Saud Univ - Sci 31:101–109. https://doi.org/10.1016/j.jksus.2017.06.004

Ritchie AM (1963) Evaluation of Rockfall and Its Control. Highw Res Rec 17, Stab Rock Slopes, Highw Res Board, Natl Res Counc Washington, DC 13–28

Rocscience (2015) Dips, v6.0. Rocscience Inc., Toronto

Romana M (1985) New Adjustment Ratings for Application of Bieniawski Classification to Slopes. In: Proceedings of the International Symposium on the Role of Rock Mechanics in Excavations for Mining and Civil Works, International Society of Rock Mechanics. Zacatecas, Mexico, pp 49–53

Roscoe KH (1970) The influence of strains in soil mechanics. Géotechnique 20:129–170. https://doi.org/10.1680/geot.1970.20.2.129

Roy P, Martha TR, Vinod Kumar K et al (2023) Cluster landslides and associated damage in the Dima Hasao district of Assam, India due to heavy rainfall in May 2022. Landslides 20:97–109. https://doi.org/10.1007/s10346-022-01977-6

Sanzeni A, Peli M, Barontini S, Colleselli F (2019) Modelling of an accidentally triggered shallow landslide in Northern Italy. Landslides 16:2277–2286. https://doi.org/10.1007/s10346-019-01251-2

Schweigl J, Ferretti C, Nössing L (2003) Geotechnical characterization and rockfall simulation of a slope: a practical case study from South Tyrol (Italy). Eng Geol 67:281–296. https://doi.org/10.1016/S0013-7952(02)00186-2

Sengupta A, Gupta S, Anbarasu K (2010) Rainfall thresholds for the initiation of landslide at Lanta Khola in north Sikkim, India. Nat Hazards 52:31–42. https://doi.org/10.1007/s11069-009-9352-9

Shan W, Xu Z, Guo Y, Zhang C (2021) Response: Commentary: the impact of climate change on landslides in Southeastern of high-latitude permafrost regions of China. Front Earth Sci 9:7. https://doi.org/10.3389/feart.2021.638578

Siddique T, Pradhan SP, Vishal V et al (2017) Stability assessment of Himalayan road cut slopes along National Highway 58, India. Environ Earth Sci 76:1–18. https://doi.org/10.1007/s12665-017-7091-x

Siddique T, Mondal MEA, Pradhan SP et al (2020) Geotechnical assessment of cut slopes in the landslide-prone Himalayas: rock mass characterization and simulation approach. Nat Hazards 104:413–435. https://doi.org/10.1007/s11069-020-04175-6

Siddque T, Pradhan SP (2018) Stability and sensitivity analysis of Himalayan road cut debris slopes: an investigation along NH-58, India. Nat Hazards 93:577–600. https://doi.org/10.1007/s11069-018-3317-9

Singh K, Kumar V (2020) Road-cut slope stability assessment along Himalayan National Highway NH-154A, India. J Geol Soc India 96:491–498. https://doi.org/10.1007/s12594-020-1587-9

Singh PK, Wasnik AB, Kainthola A et al (2013) The stability of road cut cliff face along SH-121: a case study. Nat Hazards 68:497–507. https://doi.org/10.1007/s11069-013-0627-9

Singh PK, Kainthola A, Panthee S, Singh TN (2016b) Rockfall analysis along transportation corridors in high hill slopes. Environ Earth Sci 75:1–11. https://doi.org/10.1007/s12665-016-5489-5

Singh PK, Singh KK, Singh TN (2017) Slope failure in stratified rocks: a case from NE Himalaya, India. Landslides 14:1319–1331. https://doi.org/10.1007/s10346-016-0785-4

Singh PK, Das R, Singh KK, Singh TN (2016a) Landslide in fractured and stratified rocks - A case from Aizawl, Mizoram, India. In: Proceedings of the conference on Recent Advances in Rock Engineering (RARE 2016). Atlantis Press, Paris, France, pp 375–380

Stead D (2016) The Influence of shales on slope instability. Rock Mech Rock Eng 49:635–651. https://doi.org/10.1007/s00603-015-0865-0

Tang H, Yong R, Ez Eldin MAM (2017) Stability analysis of stratified rock slopes with spatially variable strength parameters: the case of Qianjiangping landslide. Bull Eng Geol Environ 76:839–853. https://doi.org/10.1007/s10064-016-0876-4

Tawalare A (2019) Identification of risks for Indian highway construction. IOP Conf Ser Mater Sci Eng 471:102003. https://doi.org/10.1088/1757-899X/471/10/102003

Team Barak bulletin (2023) Landslide on Silchar-Haflong National Highway at Balacherra, Barak, Available online at: https://www.barakbulletin.com/en_US/landslide-on-silchar-haflong-national-highway-at-balacherra-barak-isolated-from-rest-of-assam-and-india-again-as-moonsoon-starts/

Team Business Standard (2016) Heavy landslides in Dima Hasao in Assam, May 17, 2016, Available online at: https://www.business-standard.com/article/pti-stories/heavy-landslides-in-dima-hasao-in-assam-116051701460_1.html

Team Deccan Herald (2020) 21 killed in landslides in Assam following heavy rains, June 2, 2020, Available online at: https://www.deccanherald.com/india/21-killed-in-landslides-in-assam-following-heavy-rains-844690.html

Team Northeast Now (2018) Landslides at six places in Assam's Dima Hasao, June 14, 2018, Available online at: https://nenow.in/north-east-news/landslides-at-six-places-in-assams-dima-hasao.html

Team Pratidin Time (2019) Heavy landslide at Lumding NH-27, Nov 10, 2019, Available online at: https://www.pratidintime.com/latest-assam-news-breaking-news-assam/heavy-landslide-at-lumding-nh-27

Team Times of India (2022) Silchar-Haflong Rd closed to traffic after landslides May 14, 2022, Times of India, Availbale online at: https://timesofindia.indiatimes.com/city/guwahati/silchar-haflong-rd-closed-to-traffic-after-landslides/articleshow/91552377.cms

Thuro K, Eberhardt E (2001) Landslides: causes, impacts and countermeasures adverse tunnelling conditions arising from slope instabilities—a case history. Landslides. Davos, Switzerland, pp 97–107

Umrao RK, Singh R, Singh TN (2015) Stability evaluation of hill cut slopes along National Highway-13 near Hospet, Karnataka, India. Georisk Assess Manag Risk Eng Syst Geohazards. https://doi.org/10.1080/17499518.2015.1053494

Wang G, Sassa K (2003) Pore-pressure generation and movement of rainfall-induced landslides: effects of grain size and fine-particle content. Eng Geol 69:109–125. https://doi.org/10.1016/S0013-7952(02)00268-5

Yang H, Yang T, Zhang S et al (2020) Rainfall-induced landslides and debris flows in Mengdong Town, Yunnan Province, China. Landslides 17:931–941. https://doi.org/10.1007/s10346-019-01336-y

Yoon WS, Jeong UJ, Kim JH (2002) Kinematic analysis for sliding failure of multi-faced rock slopes. Eng Geol 67:51–61. https://doi.org/10.1016/S0013-7952(02)00144-8